GKSS FORSCHUNGSZENTRUM in der HELMHOLTZ GEMEINSCHAFT

Empirical Downscaling in the Tropics – possible changes of the little rainy season (March–June) in Cameroon

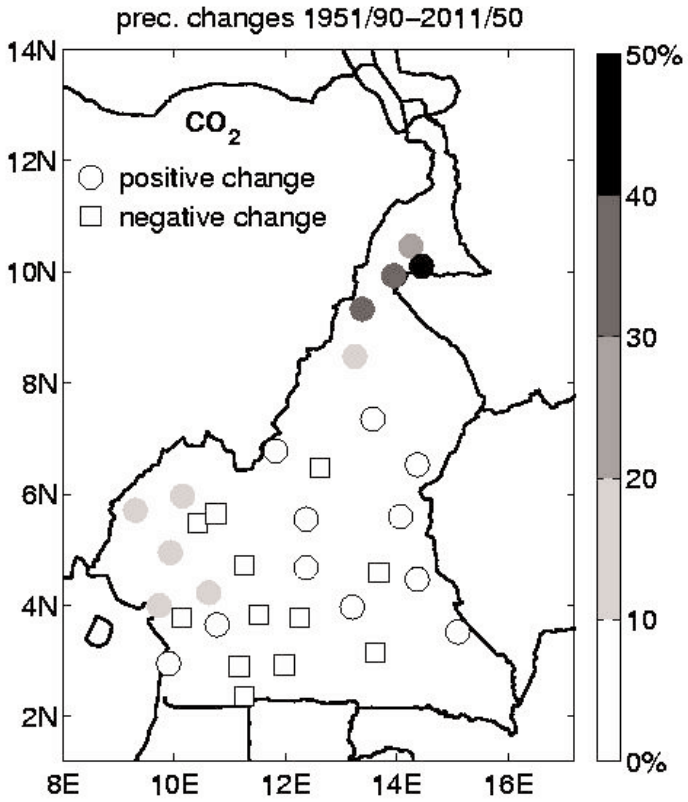

Authors:

E. K. Penlap
C. Matulla
H. von Storch
F. K. Mkankam

ISSN 0344-9629

GKSS 2003/11

GKSS 2003/11

Empirical Downscaling in the Tropics – possible changes of the little rainy season (March–June) in Cameroon

Authors:

E. K. Penlap
(Atmospheric Sciences Lab., Dep. of Physics, Faculty of Sciences, University of Yaounde I, Cameroon, and Institute for Coastal Research, GKSS Research Centre, Geesthacht, Germany)

C. Matulla
(Institute of Meteorology and Physics, University of Natural Resources and Applied Life Sciences, Vienna, Austria, and Institute for Coastal Research, GKSS Research Centre, Geesthacht, Germany)

H. von Storch
(Institute for Coastal Research, GKSS Research Centre, Geesthacht, Germany)

F. K. Mkankam
(Atmospheric Sciences Lab., Dep. of Physics, Faculty of Sciences, University of Yaounde I, Cameroon)

GKSS-Forschungszentrum Geesthacht GmbH • Geesthacht • 2003

Die Berichte der GKSS werden kostenlos abgegeben.
The delivery of the GKSS reports is free of charge.

Anforderungen/Requests:

GKSS-Forschungszentrum Geesthacht GmbH
Bibliothek/Library
Postfach 11 60
D-21494 Geesthacht
Germany
Fax.: (49) 04152/871717

ISSN 0344-9629

GKSS-Forschungszentrum Geesthacht GmbH · Telefon (04152)87-0
Max-Planck-Straße · D-21502 Geesthacht / Postfach 11 60 · D-21494 Geesthacht

GKSS 2003/11

Empirical Downscaling in the Tropics – possible changes of the little rainy season (March–June) in Cameroon

Edouard Kamdem Penlap, Christoph Matulla, Hans von Storch and François Kamga Mkankam

23 pages with 7 figures and 4 tables

Abstract

In the present work, we derive from the GCM simulated model ECHAM4/OPYC3 the changes of precipitation in Cameroon for the March-June season. Due to the presence of different climate regimes, Self-Organising Feature Maps (SOFM) is used to group stations into homogeneous rainfall regions. Then an Empirical Orthogonal Function (EOF) procedure, followed by Canonical Correlation Analysis (CCA) are used to derive statistical relationships between the homogeneous regions and large scale variables from the NCEP/NCAR reanalysis project. For the 2010-2049 horizon, the trace gas only and the trace gas plus sulphate integration induce changes, relative to the 1951–1990 climatology, ranging locally from +44 to -10 % and from +36 to -9 % respectively. Moreover the most positive changes are observed in the north and coast part of the country.

Empirisches Downscaling in den Tropen – mögliche Veränderungen der kleinen Regenzeit (März–Juni) in Kamerun

Zusammenfassung

In dieser Arbeit werden zwei Versionen des Is92a-Szenarios (Treibhausgase, Treibhausgase mit Aerosolen), die mit dem GCM ECHAM4/OPYC3 realisiert wurden, mittels empirischem Downscaling auf Stationen projiziert. Dabei betrachten wir Kamerun während der kleinen Regenzeit (März–Juni). Mit Self-Organising Feature Maps (SOFM), einer Technik der Neuronalen Netze, werden die Stationen in einem ersten Schritt in homogene Niederschlagsregionen zusammengefasst. Dann werden die Daten durch eine Hauptkomponentenanalyse (PCA) gefiltert. Mittels kanonischer Korrelationsanalyse (CCA) wird schließlich ein statistisches Modell zum Downscaling abgeleitet. In der ersten Hälfte des 21. Jahrhunderts finden wir in beiden Szenarien Ab- (bis zu -10 %) und Zunahmen (bis zu +44 %). Die größten Zunahmen werden lokal an der Küste und im Norden Kameruns erreicht.

Manuscript received / Manuskripteingang in TDB: 16. April 2003

1 Introduction

Repeated drought and famine on the African continent in the last few decades have led to a high awareness of the effect of climate variability and the potential danger of future climate change (Nicholson 1993; Hulme 1992). The North of Cameroon being in the Sahelian zone, was also hit, and the negative effects were felt in the entire country, with some shortages in agricultural produce. Because agriculture in the country is entirely rainfed and more than 90% of electricity is produced by hydropower plants, studies have been undertaken to assess vulnerability to long term climate changes that are expected to result from increase greenhouse gas (GHG) concentration in the atmosphere (IPCC 1996). These studies require projections of the possible modification of temporal and spatial pattern of local rainfall, temperature, and other important climatic variables.

General circulation climate models (GCMs) are currently the most adapted tool for these projections. However, due to their coarse resolution, 300km x 300km in the Tropics, they cannot be used for projecting local-scale changes (Grotch and MacCracken 1991). This is particularly true for surface climate variables needed for impact studies (Kamga 2000). Their resolution cannot be made much higher due to limitations in computing power and in the understanding of all the processes involved. Furthermore it is estimated that the skillful scale of GCMs is about 8 times the grid scale, therefore the GCM output on smaller scales should not be interpreted (von Storch et al. 1993; Johannesson et al. 1995). Present GCM climate projections must be converted or downscaled to higher regional or local resolutions. The leading techniques used are dynamical and statistical empirical downscaling (Hewitson and Crane 1996).

In dynamical downscaling, a limited area model (LAM) of the area of interest is nested in a GCM and evolves with it while using its output as boundary conditions (Giorgi 1990; Giorgi et al. 1994). Because of their process-based approach, LAMs are expected to generate reliable regional results, since topography, land-use patterns and other geographical features can be taken into account. In spite of their resolution being about 10 times higher than that of GCMs, in some experiments, they failed to reproduce observed precipitation statistics at spatial and temporal scales required for regional impact assessment (Giorgi 1991; Charles et al. 2001). Furthermore they are computationally expensive, and most impact assessment research groups do not have LAM.

Another strategy to overcome the gap between large and local scales is the use of empirical downscaling techniques (von Storch et al. 1993). It requires empirically linking large scale circulation patterns or variables that are well resolved and projected by GCMs, to the local climate variables of interest. A model representing the relationship between large and local scale variables is built and calibrated with observations from the current climate, and it is assumed that these relations will still hold under a changed climate.

Various methods are used, among them, regression analysis (Matulla et al. 2002), canonical correlation analysis (von Storch et al. 1993; Zorita et al. 1995) and neural network (Olsson et al. 2001). Empirical methods offer an attractive approach at significantly lower computing costs (Hewitson and Crane 1996) and it is the only way to assess the potential impacts of climate change in the Central African region since there is no LAM running in this area at the moment. However, the literature contains only a few examples of such studies in tropical Africa.

In this study, we are interested in local patterns of rainfall under a changed climate for Cameroon. Owing to its latitudinal extension, to its proximity of the Atlantic ocean and to the variety of its relief, Cameroon has a very contrasted climate and the spatial rainfall patterns are quite complex (Figure 2). Furthermore, the annual cycle of rainfall is modulated by the South-North and North-South annual migration of the Intertropical Convergence Zone (ITCZ), which marks the limit between the dry Sahelian Harmattan winds and the humid South Westerly Monsoon flow (Janowiak 1988).

The different sources of variability resulting in this spatio-temporal diversity point to the difficulties in identifying single large scale variables modulating precipitation in the whole of Cameroon. Some regionalisation studies on a monthly basis have been done in the area (Mkamkan et al. 1994) in order to access the sources of variability. Hence, we decided to regionalise the precipitation data before downscaling. In such a situation, this strategy can be benefit (Woth 2001).

2 Data

For model fitting of relations between large and local scale, we used monthly mean values of relative and specific humidity, temperature, geopotential, zonal and meridional wind, vorticity and divergence at four pressure levels (200, 500, 700, 850 hPa). Sea level pressure and sea surface temperature are also examined. The present climate is represented by the output of the NCEP/NCAR 50-year Reanalysis project, which uses a state-of-the-art analysis/forecast system to perform data assimilation using past data from 1948 to 1998 (Kalnay et al. 1996; Kistler et al. 2001). The reanalysis uses a frozen modern global data assimilation system, and a data base as complete as possible. The data assimilation (3D-Var) and the global spectral model are identical to the global system implemented operationally at NCEP on January 1995, except that the horizontal resolution is T62, about 210 km. The data used, gridded in 2.5°Lon $\times$ 2.5°Lat cells, cover the period from 1951 to 1990 and a sector from 20°W to 20°E and 20°S to 15°N (figure 1). They were downloaded from the NOAA-CIRES Climate Diagnostics Centre web site at http://www.cdc.noaa.gov/. On the local scale we use two different monthly precipitation

Table 1: List of the stations used and their geographical co-ordinates. See also Fig. 2 for spatial locations.

label	station name	lon[°]	lat[°]	alt[m]
1	MAROUA	14.25	10.45	423
2	KAELE	14.43	10.08	338
3	GUIDER	13.95	9.93	356
4	GAROUA	13.38	9.33	213
5	POLI	13.23	8.48	436
6	NGAOUNDERE	13.56	7.35	1113
7	MEIGANGA	14.33	7.16	1027
8	BANYO	11.81	6.75	1110
9	TIBATI	12.62	6.47	874
10	BETARE-OYA	14.08	5.60	805
11	YOKO	12.36	5.55	1031
12	BERTOUA	13.73	4.60	668
13	BATOURI	14.36	4.46	655
14	YOKADOUMA	15.10	3.52	640
15	LOMIE	13.61	3.16	640
16	ABONG-MBANG	13.20	3.96	693
17	NANGA-EBOKO	12.37	4.65	624
18	AKONOLINGA	12.25	3.77	671
19	SANGMELIMA	11.98	2.93	713
20	AMBAM	11.23	2.38	602
21	EBOLOWA	11.17	2.90	603
22	KRIBI	9.90	2.93	13
23	ESEKA	10.73	3.62	228
24	YAOUNDE	11.51	3.83	760
25	BAFIA	11.16	4.73	501
26	NGAMBE	10.60	4.20	650
27	EDEA	10.13	3.80	32
28	DOUALA-OBS.	9.70	4.01	10
29	NKONGSAMBA	9.93	4.95	816
30	BAFOUSSAM	10.43	5.48	1460
31	KOUNDJA	10.75	5.65	1217
32	BAMENDA	10.18	5.93	1608
33	MANFE	9.30	5.75	126

datasets. One obtained directly from the National Meteorological Service of Cameroon (NMSC), the other from the Food and Agriculture Organisation (FAO) of the United Nations. Using both fragmentary sets, it was possible to extract 33 station records, with sufficient data for the period from 1951 to 1990, with at most 2% of missings (Figure 2). In this study, we are interested in rainfall totals for the March-April-May-June (MAMJ)

period. The behaviour of large scale variables under climate change is simulated by the Max Planck Institute (MPI) für Meteorologie coupled atmosphere-ocean GCM model ECHAM4/OPYC3 (Roeckner et al. 1996), which is known to give a good representation of the climate of the region (Kamga 2000).

In the ECHAM4 experiment, performed in 1995, the horizontal resolution of the atmospheric model was 5.6° latitude by 5.6° longitude and the ocean model was 2.8° by 2.8°. Following an initialisation period of historical greenhouse gas forcing from 1860 to 1990, three simulations were done: (i) a 300-year control simulation with GHG concentrations kept at 1990 levels; (ii) a 'greenhouse gas only' forced experiment using a 1% percent annual increase in forcing from 1990 to 2099; and (iii) a 'greenhouse gas plus sulphate aerosol' integration ($CO_2 + SO_4$ aerosols) from 1990 to 2049. The 1% increase is in accordance with the IS92a emission scenario of the Intergovernmental Panel on Climate Change (IPCC 1996). The output data were interpolated to the NCEP/NCAR 2.5° × 2.5° reanalysis grid.

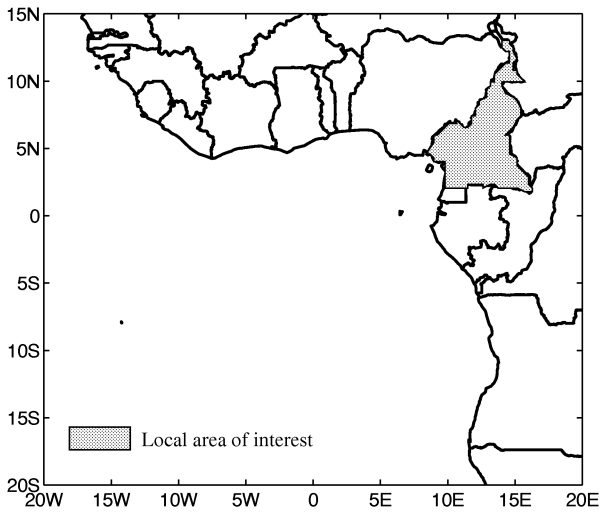

Figure 1: Local area of interest (Cameroon) and the window used for large scale variables

3 Regionalisation of precipitation - Self-Organising Feature Map

Tropical rainfall is generated by a wide variety of mechanisms, including monsoon, coastal and upper troughs, tropical cyclones, convective and advective systems, etc. Several studies have been carried out in various regions of Africa in order to link atmospheric variables to local rainfall. In Tanzania, Kabanda and Jury (1999) found that for the

period from October to December rainfall is linked to wind indices in the Indian ocean and the ENSO phase, while for the period from March to May, only rainfall in May is linked to the all-India rainfall index (Zorita and Tilya 2002). In West Africa, Sahelian rainfall was linked to sea surface temperature (Thiaw et al. 1999).

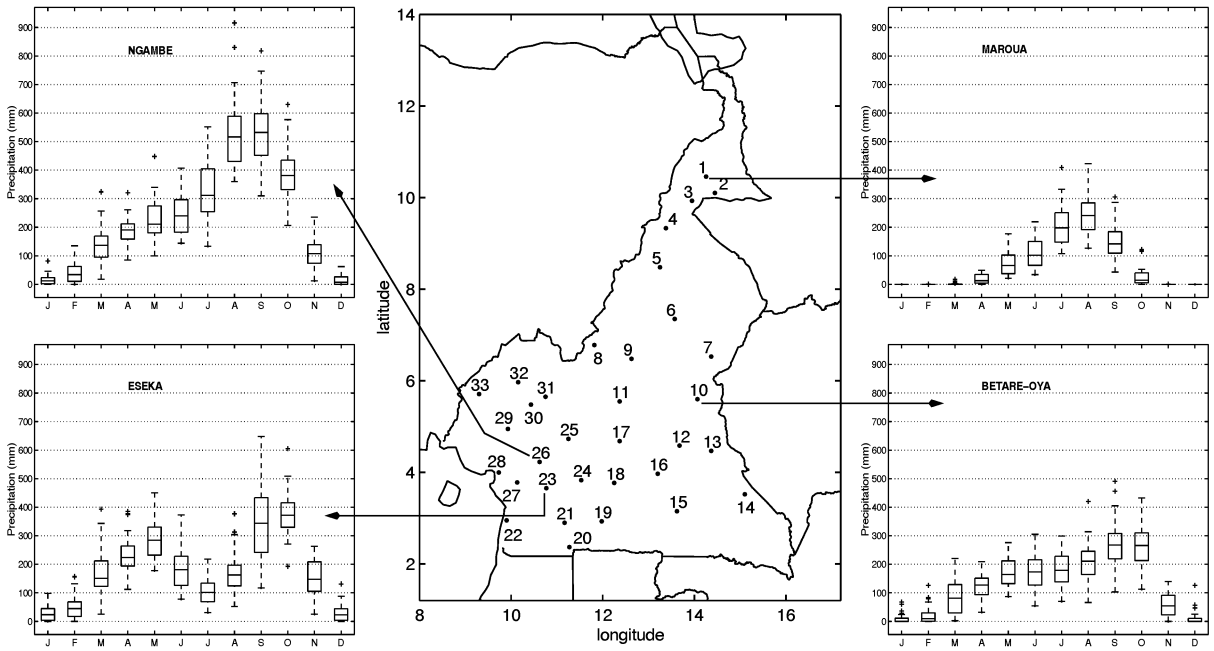

Figure 2: Stations use in this study. The panels on the left and right columns show boxplots of Monthly rainfall typical of various annual regimes in the area. Note that Ngambe (26) and Eeska (23), two neighbouring stations, quite different annual cycles while Betare-Oya (10) shows an intermediate situation

In Central Africa, the Intertropical Convergence Zone (ITCZ) is one of the phenomena affecting precipitation. In Cameroon the Adamaoua plateau and the Cameroon mountain (4100m) also affects its spatial distribution. Figure 2 shows examples of climate regimes in the region. The wet equatorial climate with four seasons (e.g. Eseka [23]), the dry Sahelian climate with two seasons (e.g. Maroua [1]) and intermediate climates (e.g. Betaré-Oya [10]) are present. Various mechanisms acting together or independently cause this complexity. From this point of view, it seems reasonable to group stations with similar properties before linking them to the general circulation. Thus different atmospheric variables can be identified as sources of rainfall variability in different regions. Among the varieties of tools available for rainfall regionalisation (e.g. cluster analysis or rotated empirical orthogonal functions), we use Self-Organising Feature Map (SOFM) because of its flexibility.

SOFMs (Kohonen 1989) are a subgroup of artificial neural networks (ANNs) used to extract significant patterns or features in the input data (Haykin 1994). This methodology

provides a mechanism for visualising any distribution of data on a two-dimensional map while preserving the statistical properties of the input distribution (Laha and Pal 2001). In the climatology domain, SOFMs have been used for classification purposes (Malmgren and Winter 1999; Cavazos 2000) and can achieve the same results as obtained by other methods. Hewitson and Crane (2002) recently used SOFM to describe changes of synoptic circulation over time and discuss in detail its performances and its utility in the climatology domain.

3.1 Application and Results of the SOFM Methodology

The architecture of SOFM in 2 dimensions consists of one output layer of $m_0 \times n_0$ nodes and one single input layer with n nodes. Each node of the output layer is connected to all nodes of the input layer through the *connection weights*. The input data are arranged as a matrix of dimensions $m \times n$, where m and n are the number of observations and variables respectively. These data are then mapped through an iterative process onto the output layer. Each iteration consists of randomly selecting an observation (input vector), finding its "best matching" node (the one having the smallest Euclidean distance to the input vector) and updating the *connection weights* not only for the best matching node, but also for nodes in its vicinity. The updating formula is a function of the *learning rate* which decreases continually during the iterations. At the end of the process, the output nodes are arranged so that observations that share similarities in the input space are mapped either through the same node or through two nodes close to each other in the output layer. Observations whose mapped nodes represent a dense area in the output layer can be interpreted as a group of data with some similar properties.

The interpretation of SOFM clusters strongly depends on the way in which the input vector is passed to the network. In the case where m denotes the length of the time series and n the number of grid points or stations, the similarity will be looked for in the time-domain, resulting in the clusters indicating various stages of evolution through the time. On the other hand, if the transposed of the data matrix is used, the similarity will be in the grid points or station-space, leading to clusters of stations or grid points in which the time series varies in a similar way. Our data were analysed in the latter mode.

The data we used are standardised seasonal anomalies of monthly precipitation from 1951 to 1990 recorded at 33 stations. Application of SOFM to the data matrix leads to assigning the various stations to the groups C1($*$), C2($\circ$) and C3($+$) displayed in Figure 3. Stations in C1 are located in the North and West of the domain and are characterised by a unimodal annual cycle. In view of the high contrast in amounts of rainfall, altitude and latitude between them, the probable linkage here is the type of circulation producing precipitation. This point will become clearer later. Stations in C3, located in the South

have a clear minimun of rainfall in May, when the Intertropical Front (ITF) is nearing its northernmost position, and the area is zone D of the ITCZ (Hamilton and Archibald 1945). Stations in C2 are in a transition zone between the preceding two.

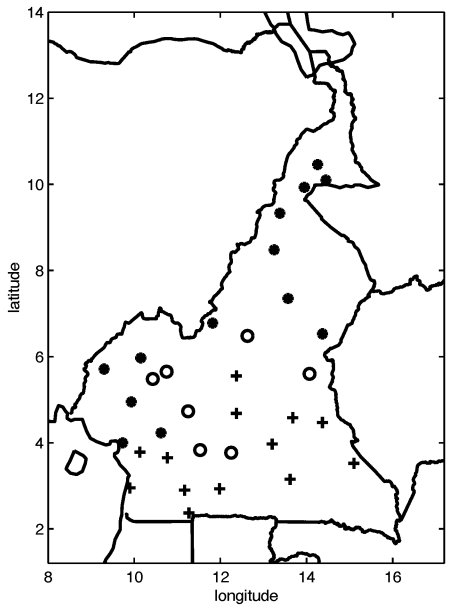

Figure 3: Clusters found by SOFM based on standardised anomalies for the period 1951-1990. C1 (∗), C2 (∘) and C3 (+).

4 Statistical Downscaling - Canonical Correlation Analysis

Downscaling in general is based on the assumption that regional climate is conditioned by climate on larger scales. Statistical Downscaling utilises observations in order to derive relationships between different scales. These relationships can be used to obtain small scale realisations from large scale climate change scenarios provided by GCMs. We use Canonical Correlation Analysis (CCA), which attempts to find optimally coupled anomaly patterns on both scales (von Storch and Zwiers 1999). CCA has found wide application to precipitation modelling: von Storch et al. (1993) apply CCA on winter Iberian rainfall; Gyalistras et al. (1994) not only on precipitation at some stations in Switzerland, but also on several other local meteorological elements as well; Busuioc and von Storch (1996) apply it on monthly Romanian precipitation amounts.

4.1 Methodology

The statistical downscaling model is constructed in two steps: First, we analyse the data on both scales using Empirical Orthogonal Function (EOF) Analysis (Lorenz 1956; Richman 1986). The aim of this step is to discriminate between the the signal of interest and the noise. This allows to obtain the most important modes of variability and to substantially reduces the data dimensionality. Secondly CCA is used to study the correlation structure between local precipitation and two large scale meteorological variables during the small rainy season, March-April-May-June (MAMJ) in Cameroon. This step is done separately for each region found by SOFM.

4.2 Application and Results

4.2.1 Model building

On both scales, the number of EOFs retained for further analysis did not exceed eight and was such that at least 80% of the total variance are retained. To detect atmospheric variables which have an influence on rainfall variability all possible combinations of two different large scale fields, as listed in the data section, were used as predictors in CCA.

In order to test the numerous models three validation experiments named A, B and C were constructed. In experiment A the (EOF-CCA) model is calibrated and validated from 1951 to 1990. In B the model is calibrated from 1951 to 1980 and validated over the whole period and in C, the calibration and the validation periods are 1951-1980 and 1961-1990, respectively. This choice is guided by the shortlength (40 years) of the time series. The experiments are carried out separately for each of the homogeneous regions found by SOFM (see Figure 3) and for the region as a whole (denoted ALL). To assess the performance of the various models, we evaluate the Pearson correlation coefficient r between the estimated and observed time series and test its significance at the 95% significance level. The best performing models are selected to downscale the GCM scenarios.

The skill of a particular predictor combination is measured by the mean of r^2 and the percentage of stations per region with significant r. In the following the percentage of stations with a significant r will be abbreviated PSR. Table 2 displays the predictors, obtained results from the previously described selection process, and their r^2 statistics for the small rainy season in Cameroon. The first column indicates the experiment, the second one the predictor-combination, the third the region, followed by columns characterising the distribution of r^2. The last column displays the percentage of stations whose correlations are significant at the 95% level (PSR $\geq$ 95%).

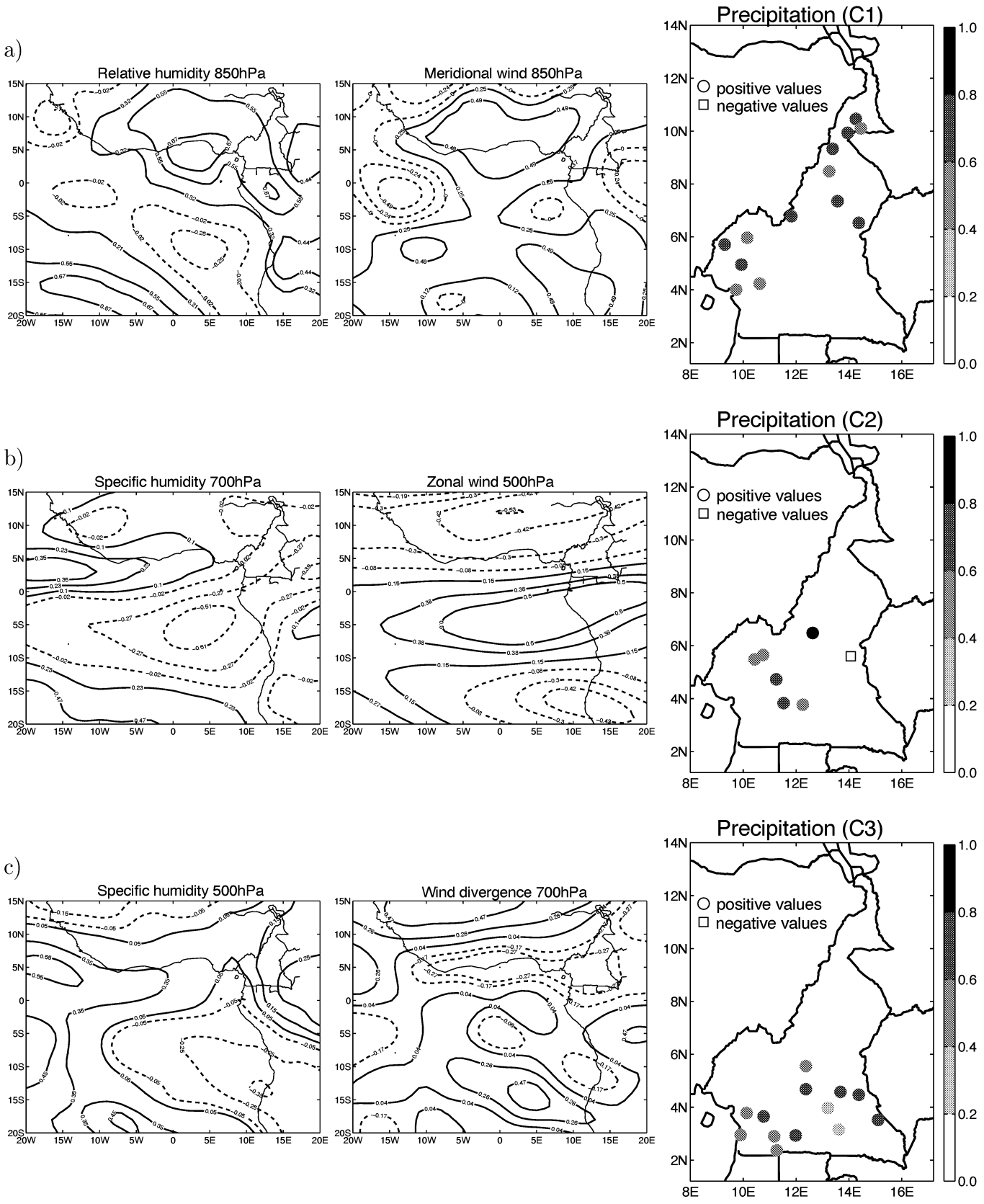

Figure 4: First CCA patterns associated with MAMJ rainfall for the SOFM defined homogeneous regions. The values are standardised. The canonical correlations between the first time coefficients are 0.88 for C1 a), 0.73 for C2 a) and 0.76 for C3 c). The names of the variables are indicated above the pictures

Table 2: Statistic of squared correlation between observed and downscaled precipitation for MAMJ. RH and SH denotes relative and specific humidity respectively, u and v the zonal and meridional winds, $divV$ and $rotV$ the wind divergence and vorticity, while the indices 8, 7, 5 represent pressure levels 850, 700 and 500hPa respectively. PSR stands for percentage of stations with a significant r.

Squared correlation r^2							
Exp.	Predictors	Region	min.	max.	mean	std.	PSR $\geq$ 95%
A	RH_8+v_8	C1	0.23	0.51	0.39	0.09	100%
	SH_7+u_5	C2	0.19	0.35	0.24	0.07	71%
	SH_5+$div\mathbf{V}_7$	C3	0.13	0.45	0.29	0.09	100%
	SH_5+$rot\mathbf{V}_5$	ALL	0.11	0.48	0.27	0.11	91%
B	RH_8+v_8	C1	0.15	0.49	0.31	0.11	100%
	SH_7+u_5	C2	0.14	0.27	0.20	0.07	71%
	SH_5+$div\mathbf{V}_7$	C3	0.16	0.50	0.31	0.11	100%
	SH_5+$rot\mathbf{V}_5$	ALL	0.10	0.49	0.27	0.11	91%
C	RH_8+v_8	C1	0.15	0.38	0.26	0.08	85%
	SH_7+u_5	C2	0.14	0.28	0.22	0.06	86%
	SH_5+$div\mathbf{V}_7$	C3	0.13	0.38	0.25	0.08	77%
	SH_5+$rot\mathbf{V}_5$	ALL	0.14	0.44	0.24	0.09	73%

4.2.2 Results and discussions

Figure 4 shows the first CCA patterns for each region. The CCA rainfall pattern in region C1 explains 37% of total variance. For comparison, the first rainfall EOF in C1 (not shown) explains 43% of total variance.

On the large scale (Fig. 4a) the area is under the strong influence of a positive poles of relative humidity and northerly wind located around 5°N westwards of Cameroon, and on the 850hPa level. The meridional wind intensity increases northwards up to 5°N, then quickly decreases and is reversed around 13°N. The positive pole of relative humidity can be interpreted as persistent presence of humid airmasses advected from the Atlantic ocean. Hence, deep convection producing precipitation in C1 results from moisture advection by the monsoonal flow. This possible connection was further explored by means of a composite analysis involving local precipitation, large scale relative humidity and meridional wind. The upper two panel-rows in Figure 5 show the result of the analysis. COMPOSITE+ is for the large scale composites made up of years having exceptionally high precipitation totals during the SRS. COMPOSITE- corresponds to the opposite

situation, i.e. years having considerably lesser precipitation sums during the SRS. The composite analysis supports the interpretation given above, as the composites related to high precipitation are similar to those related to low precipitation but with a reversed sign.

In C3 a situation comparable to that in C1 is found. The CCA (Fig. 4c) and COMPOSITE patterns of specific humidity at 500hPa and the wind divergence at 700hPa (Fig. 5 lower panels) show many similarities. In COMPOSITE+ there is wind convergence around 5°N and relative humidity has a positive pole above Cameroon. This combination feeds convection and can explain enhanced precipitation recorded in C3. The COMPOSITE-, which is connected to drier episodes, show positive divergence around the region of interest. Altogether these observations point to convective phenomenon as source of rain in this area.

The CCA patterns of specific humidity at 700hPa and zonal wind at 500hPa (Fig. 4b) show a complex situation in the case of C2 whit a south-north dipole for zonal wind and a east-west dipole for specific humidity around the Equator. These patterns do not allow a simple interpretations and no further investigation has been made. Furthermore, findings of Table 2 report that rainfall in C2 is insufficiently linked to large scale circulations.

In all cases it can be observed that the atmospheric signal influencing precipitation in Cameroon acts around 5°N.

The CCA models as calibrated in experiment A was used to downscale rainfall under the present climate. Figure 6 displays a direct comparison between observed and downscaled rainfall anomalies for each region. It appear that the CCA-models captures the variability of precipitation in C1 and C3 relatively well, although extreme values in C3 are underestimated. However, the trend is well reproduced in both regions. Again it can be seen that there are difficulties in C2 where the results are poorer.

To assess the benefit of regionalising precipitation data using SOFM before downscaling we used the explained variance $1 - \frac{\langle X - \hat{X} \rangle^2}{\langle X \rangle^2}$ to compare the performance of the models run with and without regionalisation. X and $\hat{X}$ are the observed and downscaled samples, respectively.

Table 3 shows the explained variance averaged over each region. For this comparison the number of EOFs retained is 8 for the large scale field and 3 for local rainfall in C2 as well as 6 in C1, C1&2, C3 and C2&3 respectively. The most striking features are: (i) The explained variances in C1 and C3 are higher than in ALL. This remains also valid when C2 is added to C1 or C3. (ii) The models calibrated for the different regions explain always a higher fraction of variance, than the models calibrated for the whole Cameroon.

So we conclude that regionalisation of rainfall data improves the model performance in regions C1 and C3 the, but is of no help in region C2. Moreover C2 could be interpreted

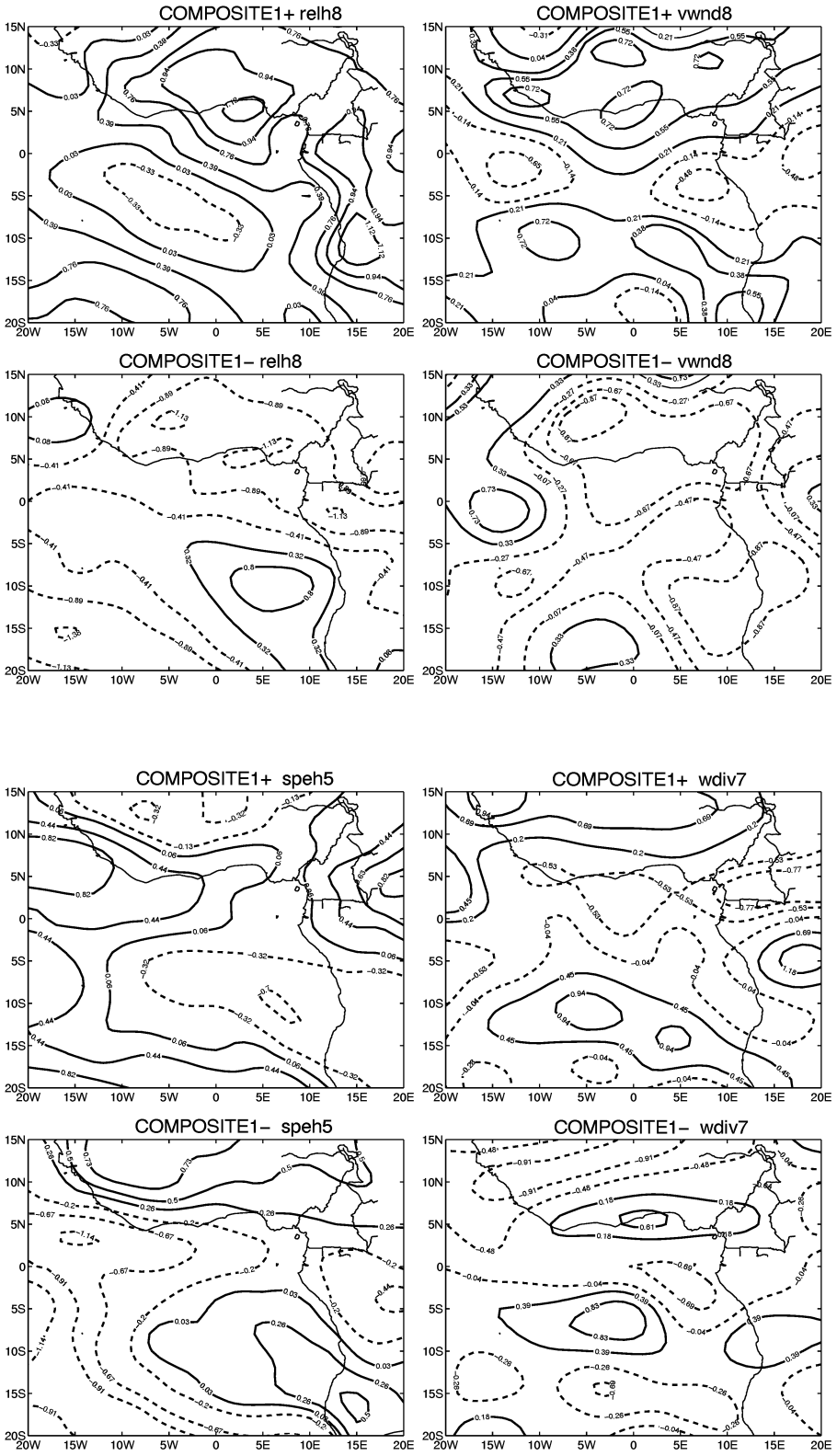

Figure 5: Composite patterns of predictor variables for region C1 (upper four panel) and C3 (lower four panel). COMPOSITE+ (COMPOSITE-) is the mean state made up of the six highest (lowest) values of the canonical time series.

as a border-region between C1 and C3. Hence, local precipitation is better represented when running CCA separately for each region found by SOFM analysis.

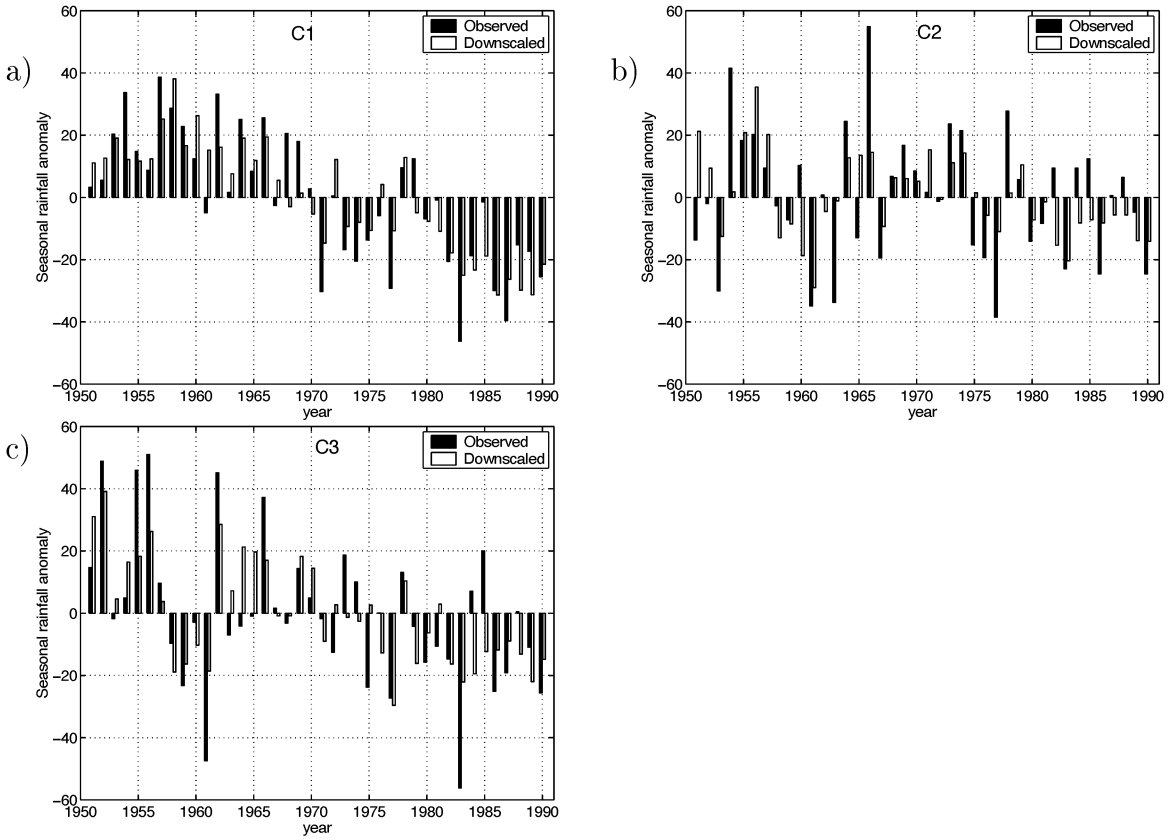

Figure 6: Time series of MAMJ rainfall averaged over the homogeneous regions a) C1, b) C2 and c) C3. (Black bars, observed; white bars estimated from experiment A)

Table 3: Model performance with regionalisation C1, C2, and C3 and without (All). The values are explained variance averaged over each region and A, B, C are the experiments performed (see text). Note: Cα in ALL denotes the model perfomance in region α based on the model fitted for ALL.

Exp.	C1	C1&2	C1 in ALL	C1&2 in AL	C2	C2 in ALL	C3	C2&3	C3 in ALL	C2&3 in ALL	ALL
A	0.39	0.31	0.36	0.29	0.17	0.16	0.27	0.22	0.25	0.21	0.23
B	0.30	0.25	0.21	0.25	0.13	0.13	0.30	0.23	0.27	0.22	0.22
C	0.22	0.19	0.22	0.18	0.20	0.09	0.18	0.17	0.17	0.16	0.17

4.2.3 Downscaled local rainfall under climate change

The transfer functions derived from EOF-CCA approach (as previously shown) are used to assess local precipitation changes for a future period.

The GCM experiments used are the ECHAM4/OPYC3 (Roeckner et al. 1996) as

described earlier. Two IS92a scenarios are investigated; the 'greenhouse gas only' run for the period 2011 to 2050 and the 'greenhouse gas plus sulphate aerosols' run for 2010 to 2049. The anomalies are derived by subtracting climatological mean values, 1951-1990, calculated from the control experiment, from the effective values of the scenario runs. The anomalies are further normalised by the NCEP/NCAR reanalysis data standard deviation for 1951-1990. The models used were calibrated with the set-up described in experiment A. Table 4 shows (in %)the differences between the climatological values for the observed period 1951-1990 and the projection values for the periods 2011-2050 (CO_2) as well as 2010-2049 ($CO_2 + SO_4$).

Table 4: Statistic of downscaled local rainfall changes derived from a GCM experiment under IPCC IS92a scenario with CO_2 only and $CO_2 + SO_4$. Changes are expressed in percentage relative to the observed period 1951-1990.

Region	(CO_2)				($CO_2 + SO_4$)			
	min	max	mean	std	min	max	mean	std
C1	4.00	43.91	18.60	11.97	3.32	35.04	14.37	9.29
C2	-9.84	1.22	-3.99	3.49	-8.24	0.89	-3.38	2.82
C3	-1.58	0.78	-0.09	0.63	-1.26	1.48	0.43	0.68

The statistics describe each region separately. Figure 7 shows the spatial distribution of precipitation changes induced by the CO_2 and the $CO_2 + SO_4$ scenarios. The changes are expressed in percentage relative to the observed period 1951-1990. The largest changes appear in region C1 (up to 44% increase). The rest of the country (i.e. in C2 and C3), shows both positive (increase) and negative (decrease) precipitation changes ranging from -10 to 10%. The results induced by the $CO_2 + SO_4$ scenario look quite similar to those of the CO_2 only scenario with differences in magnitude up to 8%.

The expected enhancement of precipitation in C1 could induced positive repercussions on the monthly discharge of the Upper Benue River in north of Cameroon with a direct impacts on agricultural and human activities (Kamga 2001). Overall, most of these changes may not be significant in view of GCM and downcaling models uncertainty, and furthermore, would be within current climate variability levels.

5 Conclusion

The results of Self-Organising Feature Map (SOFM) indicate that March-June precipitation (SRS) is subdivided into three groups. These groups are linked to different modes of

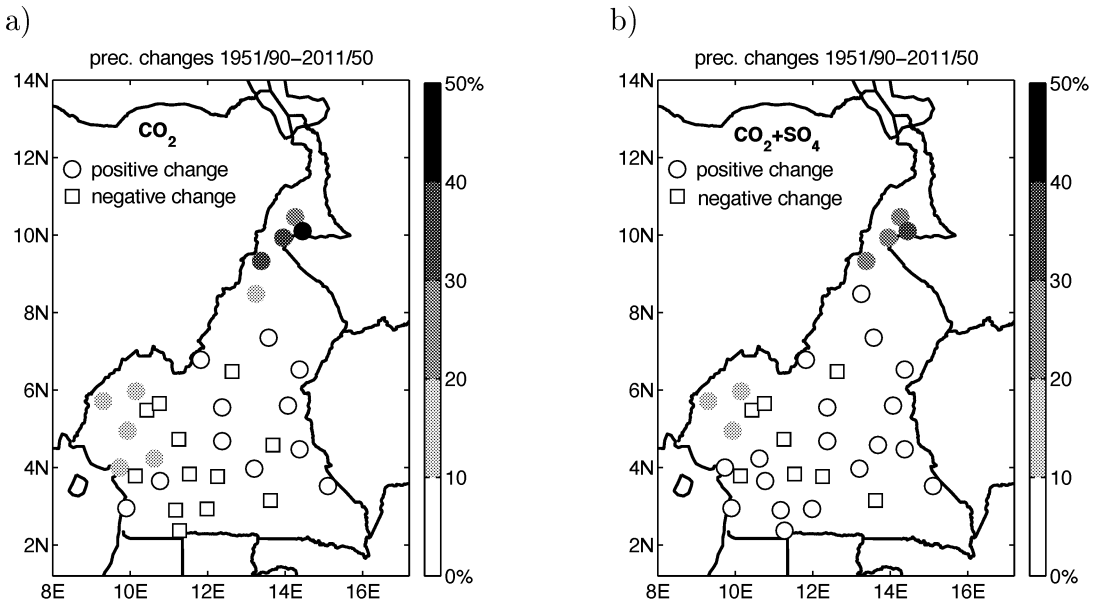

Figure 7: Downscaled local rainfall changes derived from a GCM experiment under IPCC IS92a scenario: a) CO_2 only; b $CO_2 + SO_4$. Changes are expressed in percentage relative to the observed period 1951-1990.

variability, which might be related to different atmospheric mechanisms. Results of the EOF and CCA techniques show that in part of the study domain relative humidity and meridional wind at 850hPa influence the local precipitation during the SRS. A composite analysis suggests that this might be due to advective processes. In the southern part of Cameroon, the combination of 500hPa specific humidity and 700hPa wind divergence is linked best to the variability of local precipitation. In this case the composite analysis indicate a connection between rainfall and convective phenomena. Projection of future precipitation based on two IS92a emission scenarios as simulated by ECHAM4/OPYC3 indicate trace gas only and trace gas plus sulphate integration induce changes, relative to the 1951-1990 climatology, ranging locally from +44 to -10% and from +36 to -9%, respectively.

This study demonstrates the possibility of downscaling of local scale climate change scenarios from GCMs in Cameroon. The presented approach offers a possible strategy to produce these scenarios at low computing costs. Cameroon's climate runs from humid-equatorial close to the Atlantic ocean to arid-tropical in the vicinity of the lake Chad, in the Sahelian zone. Hence the achieved results may be useful for neighbouring area in Central Africa.

6 Acknowledgments

We thank the DKRZ, the FAO and the NMSC for providing data. Moreover we would like to thank E. Zorita, S. Wagner and C. Nunneri for fruitful discussions that help to improve the manuscript. E. K. Penlap would further thanks the German Co-operation Agency DAAD, for granting him a fellowship and Prof. Hans von Storch for welcoming him in his Laboratory.

References

Busuioc, A., and H. von Storch, 1996: Changes in the winter precipitation in Romania and its relation to the large-scale circulation. *Tellus*, **48A**, 538–552.

Cavazos, T., 2000: Using Self-organizing maps to investigate extreme climate events: An application to wintertime precipitation in the balkans. *J. Climate*, 1718–1732.

Charles, S.P., B.C. Bates, S.J. Crimp, and J.P. Hughes, 2001: Statistical Downscaling of daily, multi-site, precipitation in tropical and sub-tropical climates. In: *8th International Meeting on Statistical Climatology*. University of Lüneburg, Germany.

Giorgi, F., 1990: Simulation of regional climate using a limited area model nested in a general circulation model. *J. Climate*, **3**, 941–963.

Giorgi, F., 1991: Sensitivity of simulated summertime precipitation over the Western United States to different physics parameterizations. *Mon. Wea. Rev.*, **119**, 2870–2888.

Giorgi, F., C. Shields Brodeur, and G.T. Bates, 1994: Regional climate-change scenarios over the United-States produced with a nested regional climate model. *J. Climate*, **7**, 375–399.

Grotch, S.L., and M.C. MacCracken, 1991: The use of general circulation models to predict regional climatic change. *J. Climate*, **4**, 286–303.

Gyalistras, D., H. von Storch, A. Fischlin, and M. Beniston, 1994: Linking GCM-simulated climatic changes to ecosystem models: case studies of statistical downscaling in the Alps. *Clim. Res.*, **4**, 167–189.

Hamilton, R.A., and J.W. Archibald, 1945: Meteorology of Nigeria and adjacent territory. *Quart. J. Roy. Meteor. Soc.*, **71**, 231–264.

Haykin, S., 1994: *Neural Networks: A Comprehensive Foundation*. Macmillan College Publishing Company.

Hewitson, B., and R. Crane, 1996: Climate downscaling: techniques and application. *Clim. Res.*, **7**, 85–95.

Hewitson, B.C., and R.G. Crane, 2002: Self-organizing mags: applications to synoptic climatology. *Clim. Res.*, **22**, 13–26.

Hulme, M., 1992: Rainfall changes in Africa - 1931-1960 to 1961-1990. *Int. J. Climatol.*, **7**, 685–699.

IPCC, 1996: *Climate Change 1995 - The Science of Climate Change; Contribution of Working Group I to the Second Assessment Report of the Intergovernmental Panel on Climate Change*. Cambridge University Press, 572 pp.

Janowiak, E.J., 1988: An Investigation of Interannual Rainfall Variability in Africa. *J. Climate*, **1**, 240–255.

Johannesson, T., T. Jonsson, E. Källen, and E. Kaas, 1995: Climate change scenarios for the nordic countries. *Clim. Res.*, **5**, 181 – 195.

Kabanda, T.A., and M.R. Jury, 1999: Inter-annual variability of short rains over northern Tanzania. *Clim. Res.*, **13**, 231–241.

Kalnay, E., M. Kanamitsu, R. Kistler, W. Collins, D. Deaven, L. Gandin, M. Iredell, S. Saha, G. White, J. Woollen, Y. Zhu, M. Chelliah, W. Ebisuzaki, W. Higgins, J. Janowiak, K.C. Mo, C. Ropelewski, J. Wang, A. Leetmaa, R. Reynolds, R. Jenne, and D. Joseph, 1996: The NCEP/NCAR reanalysis project. *Bull.Amer.Meteor.Soc*, **77**, 437–471.

Kamga, F.M., 2000: Validation of general circulation climate models and projections of temperature and rainfall changes in Cameroon and some of its neighbouring areas. *Theor. Appl. Climatol.*, **67**, 97–107.

Kamga, F.M., 2001: Impact of greenhouse gas induced climate change on the runoff of the Upper Benue River (Cameroon). *Journal of Hydrology*, **252**, 145–156.

Kistler, R., E. Kalnay, W. Collins, S. Saha, G. White, J. Woollen, M. Chelliah, W. Ebisuzaki, M. Kanamitsu, V. Kousky, H. van den Dool, R. Jenne, and M. Fiorino, 2001: The NCEP-NCAR 50-Yaer Reanalysis: Monthly Mean CD-ROM and Documentation. *Bull. Amer. Meteor. Soc.*, **82**, 247–267.

Kohonen, T., 1989: *Sel-Organization and associative memory* (3 ed.). Springer-Verlag.

Laha, A., and N.R. Pal, 2001: Dynamic generation of prototypes with self-organizing feature maps for classifier design. *Pattern Recognition*, **34**, 315–321.

Lorenz, E.N., 1956: Empirical orthogonal functions and statistic weather prediction. *Sci. Rept. No. 1, Statistical Forecasting Project, Mass. Inst. Tech., Dept. of Meteorology, Cambridge, Mass.*, 49pp.

Malmgren, B.A., and A. Winter, 1999: Climate zonation in Puerto Rico based on principal components analysis and an artificial neural network. *J. Climate*, **12**, 977–985.

Matulla, C., N. Groll, H. Kromp-Kolb, H. Scheifinger, M.J. Lexer, and M. Widmann, 2002: Climate change scenarios at Austrian National Forest Inventory sites. *Clim. Res.*, **22**, 161–173.

Mkamkan, K.F., M. Tsalefac, and B.C. Mbane, 1994: Variabilité Pluviométrique sur le Territoire Camerounais: Essai de Régionalisation à Partir des Cumuls Mensuels

et du Cycle Annuel. *Publications de l'Association Internationale de Climatologie*, **7**, 439–446.

Nicholson, S.E., 1993: An Overview of African Rainfall Fluctuation of the Last Decade. *J. Climate*, **6**, 1463–1466.

Olsson, J., C.B. Uvo, and K. Jinno, 2001: Statistical Atmospheric Downscaling of Short-Term Extreme Rainfall By Neural Networks. *Phys. Chem. Earth (B)*, **26**, 695–700.

Richman, M.B., 1986: Rotation of principal components. *Int. J. Climatol.*, **6**, 293–335.

Roeckner, E., J. Oberhuber, A. Bacher, M. Christoph, and I. Kirchner, 1996: ENSO varability and atmospheric response in a global coupled atmosphere-ocean GCM. *Climate Dyn.*, **12**, 737–745.

Thiaw, W.M., G.A. Barnston, and V. Kumar, 1999: Predictions of African rainfall on the seasonal timescale. *J. Geophys. Res.*, **104**, 31589–31597.

von Storch, H., E. Zorita, and U. Cubasch, 1993: Downscaling of global climate change estimates to regional scales: An application to iberian rainfall in wintertime. *J. Climate*, **6**, 11161 – 11171.

von Storch, H., and F. Zwiers, 1999: *Statistical Analysis in Climate Research*. Cambridge University Press, 528 pp.

Woth, K., 2001: Abschätzung einer zukünftigen Niederschlagsentwicklung mit statistischen Methoden unter Einbezug räumlicher Differenzierungsverfahren am Beispiel des südwesteuropäischen Raums. Master's thesis, GKSS-Report 2001/28 - University of Trier, 101 pp.

Zorita, E., J.P. Hughes, D.P. Lettemaier, and H. von Storch, 1995: Stochastic characterization of regional circulation patterns for climate model diagnosis and estimation of local precipitation. *J. Climate*, **8**, 1023–1042.

Zorita, E., and F.F. Tilya, 2002: Rainfall variability in Northern Tanzania in the March-May season (long rains) and its links to large-scale climate forcing. *Clim. Res.*, **20**, 31–40.